

# Characterization of an Extensive Transverse Tubular Network in Sheep Atrial Myocytes and its Depletion in Heart Failure

Katharine M. Dibb, PhD; Jessica D. Clarke, PhD; Margaux A. Horn, BSc; Mark A. Richards, PhD; Helen K. Graham, PhD; David A. Eisner, DPhil; Andrew W. Trafford, PhD

**Background**—In ventricular myocytes, the majority of structures that couple excitation to the systolic rise of  $\text{Ca}^{2+}$  are located at the transverse tubular (t-tubule) membrane. In the failing ventricle, disorganization of t-tubules disrupts excitation contraction coupling. The t-tubule membrane is virtually absent in the atria of small mammals resulting in spatiotemporally distinct profiles of intracellular  $\text{Ca}^{2+}$  release on stimulation in atrial and ventricular cells. The aims of this study were to determine (i) whether atrial myocytes from a large mammal (sheep) possess t-tubules, (ii) whether these are functionally important, and (iii) whether they are disrupted in heart failure.

**Methods and Results**—Sheep left atrial myocytes were stained with di-4-ANEPPS. Nearly all control cells had an extensive t-tubule network resulting in each voxel in the cell being nearer to a membrane (sarcolemma or t-tubule) than would otherwise be the case. T-tubules decrease the distance of 50% of voxels from a membrane from  $3.35 \pm 0.15$  to  $0.88 \pm 0.04 \mu\text{m}$ . During depolarization, intracellular  $\text{Ca}^{2+}$  rises simultaneously at the cell periphery and center. In heart failure induced by rapid ventricular pacing, there was an almost complete loss of atrial t-tubules. The distance of 50% of voxels from a membrane increased to  $2.04 \pm 0.08 \mu\text{m}$ , and there was a loss of early  $\text{Ca}^{2+}$  release from the cell center.

**Conclusion**—Sheep atrial myocytes possess a substantial t-tubule network that synchronizes the systolic  $\text{Ca}^{2+}$  transient. In heart failure, this network is markedly disrupted. This may play an important role in changes of atrial function in heart failure. (*Circ Heart Fail.* 2009;2:482-489.)

**Key Words:** atrium ■ calcium ■ cells ■ heart failure ■ t-tubules

The atria play an important role in assisting ventricular filling. Atrial fibrillation is the most common cardiac arrhythmia.<sup>1</sup> However, much less is known about the regulation of calcium ( $\text{Ca}^{2+}$ ) and excitation-contraction coupling in the atrium than in the more widely studied ventricle. As in the ventricle, atrial contraction is initiated by opening of voltage gated L-type  $\text{Ca}^{2+}$  channels ( $I_{\text{Ca-L}}$ ) triggering release of  $\text{Ca}^{2+}$  from the intracellular  $\text{Ca}^{2+}$  store, the sarcoplasmic reticulum thus giving rise to the systolic  $\text{Ca}^{2+}$  transient.<sup>2</sup> The ventricle contains regular invaginations in the surface membrane (t-tubules) on which are concentrated many of the proteins involved in excitation-contraction coupling. T-tubules allow close coupling of  $\text{Ca}^{2+}$  entry via  $I_{\text{Ca-L}}$  and  $\text{Ca}^{2+}$  release from the sarcoplasmic reticulum store thus ensuring a rapid and synchronous rise in  $[\text{Ca}^{2+}]_i$  and thus contraction of the cell (for review, see reference 3). T-tubules are much less evident in atrial cells<sup>4,5</sup> appearing to be virtually absent from atrial cells from both rat and cat.<sup>6,7</sup> However, in some cases, a limited axial (often longitudinal) tubular structure has been found in the rat atrium and demonstrated to facilitate  $\text{Ca}^{2+}$  release from the sarcoplasmic reticulum.<sup>8,9</sup> It is important to

note in these cases that the structure of the t-tubule network is very different to that in the ventricle.

## Clinical Perspective on p 489

One consequence of a lack of t-tubules in atrial myocytes is that on depolarization, the initial rise in  $\text{Ca}^{2+}$  occurs only at the cell periphery and spreads into the center of the cell by propagation as a wave of  $\text{Ca}^{2+}$  induced  $\text{Ca}^{2+}$  release.<sup>6,10–12</sup> Similar radially propagating  $\text{Ca}^{2+}$  waves are produced in ventricular cells by formamide-induced disconnection of the t-tubule from the surface sarcolemma (detubulation)<sup>13</sup> emphasizing the role of the t-tubule in synchronization of the systolic  $\text{Ca}^{2+}$  transient.<sup>6,12</sup>

The majority of studies on atrial cells have been performed on small mammals (eg, rat and cat<sup>6,11,14,15</sup>). In contrast, larger species are required for studies of atrial fibrillation in order that atrial fibrillation can be maintained. The goat,<sup>16</sup> sheep,<sup>17</sup> and dog<sup>18</sup> have been used extensively for this purpose. However, we could find no data in the literature on the ultrastructure of atrial cells from either sheep or goat. As far as the dog is concerned, a single article reports the presence

Received January 20, 2009; accepted July 9, 2009.

From the Unit of Cardiac Physiology, University of Manchester, Core Technology Facility, Manchester, United Kingdom.

Correspondence to Katharine M. Dibb, PhD, Unit of Cardiac Physiology, University of Manchester, Core Technology Facility, 46 Grafton St, Manchester M13 9NT, United Kingdom. E-mail [katharine.dibb@man.ac.uk](mailto:katharine.dibb@man.ac.uk)

© 2009 American Heart Association, Inc.

*Circ Heart Fail* is available at <http://circheartfailure.ahajournals.org>

DOI: 10.1161/CIRCHEARTFAILURE.109.852228

of t-tubules in the atrium.<sup>19</sup> These tubules were more obvious in the interatrial band compared with the wall of the atrium. However, the study used multicellular sections, and it was impossible to quantify the density of tubules. A more recent study found t-tubules in canine atrial myocytes<sup>20</sup> although any role in excitation-contraction coupling was not considered.

Several studies have shown disruption to the ventricular t-tubular system in heart failure leads to dysynchrony of the systolic  $\text{Ca}^{2+}$  transient.<sup>21–24,28</sup> It is unknown, however, if atrial t-tubules are affected in heart failure. The aim of this work was therefore to examine (1) the distribution of transverse tubules in the sheep atrium and (2) whether this is altered in heart failure? We find a well developed t-tubular structure in normal sheep atrial myocytes. Associated with this, we also find that the systolic  $\text{Ca}^{2+}$  transient can develop in the interior of the atrial myocyte without the need for propagation from the periphery. In addition t-tubules virtually disappear in failing atrial myocytes, and this is accompanied by dependence of the  $\text{Ca}^{2+}$  transient on propagation from periphery to interior. These findings have considerable significance for our understanding of the regulation of atrial contraction.

## Methods

All procedures accord to the United Kingdom Animals (Scientific Procedures) Act of 1986.

### Cell Isolation

Cells were isolated from the left atrium of sheep using a collagenase and protease digestion technique. Animals were heparinized (10 000 IU intravenously) and euthanized with an overdose of pentobarbitone (200 mg/kg intravenously). The heart was removed and atria and ventricles separated. The left superior atrial artery was cannulated, and the atria perfused with nominally  $\text{Ca}^{2+}$  free solution for 10 minutes. The  $\text{Ca}^{2+}$  free solution contained (in mmol/L) NaCl, 134; glucose, 11; HEPES, 10; 2,3-butanedione monoxime (BDM), 10; KCl, 4;  $\text{MgSO}_4$ , 1.2;  $\text{NaH}_2\text{PO}_4$ , 1.2 and 0.5 mg/mL bovine serum albumin (BSA); pH 7.34 with NaOH. Collagenase (Worthington type II, 0.55 mg/mL) and protease (type XIV, 0.06 mg/mL) were then added to the  $\text{Ca}^{2+}$  free solution and perfused for approximately 12 minutes. The atria were then perfused with a taurine solution (in mmol/L): NaCl, 113; taurine, 50; glucose, 11; HEPES, 10; BDM, 10; KCl, 4;  $\text{MgSO}_4$ , 1.2;  $\text{Na}_2\text{HPO}_4$ , 1.2;  $\text{CaCl}_2$ , 0.1; and BSA 0.5 mg/mL (pH 7.34 with NaOH) for 20 minutes. The left atrial free wall and left atrial appendage were then dissected free and cells isolated from each region by gentle trituration. Cells were stored in taurine solution until use. Sheep left ventricular and rat atrial cells were isolated as previously described.<sup>15,25</sup>

### Heart Failure

Animals were anesthetized with isoflurane in oxygen, intubated and ventilated at 15 breaths per minute throughout the surgical procedure. Perioperative analgesia was provided with meloxicam (0.5 mg/kg SC) and antibiotics with enrofloxacin (2.5 mg/kg SC). Two IS-1 (St Jude Medical) active fixation endocardial pacing leads were fixed at the apex of the right ventricle via a transvenous approach and connected to a Medtronic Thera pacemaker secured in a cervical subcutaneous pocket. Animals were allowed to recover from surgery for 10 to 14 days before rapid right ventricular pacing was activated at 210 beats per minute of 4 weeks duration.

Echocardiography was performed on conscious supine animals using a 1 to 5 MHz linear phased array probe (Sonosite) before surgical implantation of the pacemaker and immediately before sacrifice.

## Confocal Microscopy

The point spread function (PSF) of the imaging system (63×1.2 numeric aperture water immersion lens on a Leica SP2 confocal) was obtained using 100 nm diameter polystyrene beads (Molecular Probes) imaged at an x-y resolution of 100 nm and vertical z stacks of 162 nm separation as described previously.<sup>15,26</sup> Fluorescence was excited at 488 nm and emitted light collected >515 nm. Cells were imaged in the same manner as the beads. Images of the surface membrane and t-tubules were obtained by staining with di-4-ANEPPS (Molecular Probes) at a final concentration of 2  $\mu\text{mol/L}$ . Measurements were begun approximately 2 minutes after adding the indicator and continued for 15 minutes. We found that longer exposure to di-4-ANEPPS sometimes resulted in its intracellular accumulation. For measurements of  $[\text{Ca}^{2+}]_i$ , cells were loaded with either Fluo-5F or Fluo-3 AM (5  $\mu\text{mol/L}$  for 10 minutes). Fluorescence was excited at 488 nm and emitted light collected at 515 to 600 nm. The experimental perfusate for intracellular  $\text{Ca}^{2+}$  measurements contained (in mmol/L): NaCl, 140; HEPES, 10; glucose, 10; KCl, 4;  $\text{MgCl}_2$ , 1;  $\text{CaCl}_2$  1.8. pH 7.34 with NaOH. Cells were stimulated by a pair of silver field electrodes at 0.5 Hz. All experiments were performed at 23°C.

## Image Analysis

Even when using confocal microscopy, the resolution of images is limited by the effects of blurring due to out of focus fluorescence.<sup>26</sup> We therefore used a deconvolution algorithm and the PSF of the imaging system (Huygens Essential, Scientific Volume Imaging) to correct this problem.<sup>15</sup> To calculate the distance of points in the cell from the nearest membrane, we wrote routines in IDL (RSI Inc). (1) The images were thresholded using a value 30% greater than the mean value of the fluorescence from the section thus ensuring that membranes were bright and the rest dark. (2) Images were resampled to make the z spacing the same as the x-y (IDL routine “congrid”), and then the distance of the nearest membrane from any point was calculated (IDL routine “morph\_distance”). (3) Blank sections were added above and below the z stack (“padding”) to ensure that the distance map did not suffer from artifacts due to absence of data above and below the cell. In some figures, the distance of points to the nearest surface membrane and t-tubule were calculated separately. In each case, the distance to surface sarcolemmal or t-tubule membrane was calculated for the central z-sections of the cell, avoiding the top and bottom surfaces. The distance to the nearest surface membrane was obtained by replacing the cell image with its outline calculated in IDL. (1) Any fluorescent objects outside the cell were removed by editing images in ImageJ (National Institutes of Health). (2) The program scanned along each horizontal line from left to right. The first bright pixel reached was identified as part of the left hand border of the cell and the last bright pixel as part of the right hand border. (3) Scanning down each vertical line similarly gave the top and bottom borders of the cell. Sometimes no bright point was seen, and the cell outline therefore had small discontinuities. We estimate that these would produce a trivial error in calculating the distance to the nearest surface membrane. The distance to the t-tubules was obtained by removing the surface membrane from the images. Here, it was important that there be no discontinuities in the calculated surface membrane therefore small discontinuities were eliminated in ImageJ. These surface membrane images were convolved with the whole section to remove the surface membrane.

## Statistics

All data are presented as mean  $\pm$  SE (SEM) or median and interquartile range. Data have been compared using a Student *t* test, paired *t* test, or Mann-Whitney Rank Sum test (where either the data were not normally distributed or had unequal variance). Data were considered significant when  $P < 0.05$ .

## Results

### Sheep Atrial Myocytes Have Extensive T-Tubule Structure

All of the 42 sheep atrial cells studied contained t-tubules. Figure 1 shows typical planar (x-y) confocal sections from

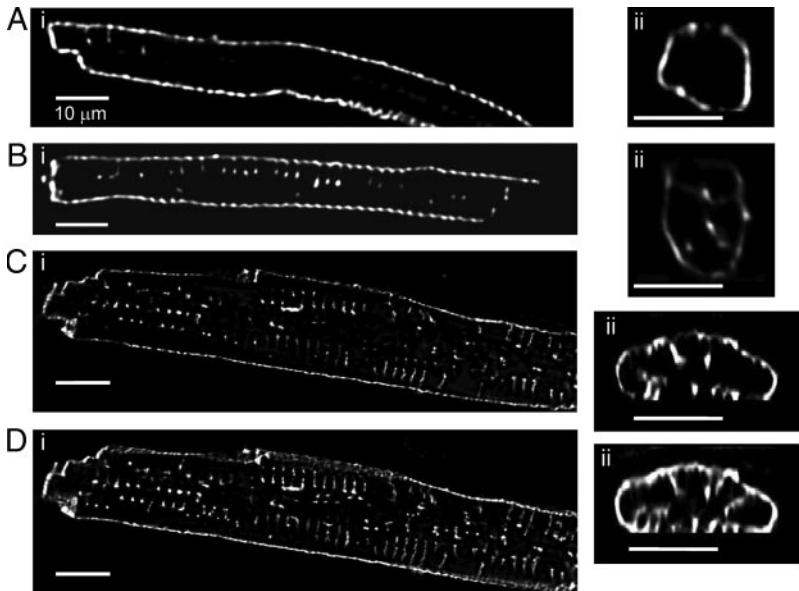


**Figure 1.** Specimen deconvolved images of cell membranes of sheep atrial myocytes. A–C, 3 cells. Each panel shows a xy image (i) and a reconstructed yz image (ii) at one point in the cell. D, 2- $\mu\text{m}$ -thick projections. All scale bars are 10  $\mu\text{m}$ .

sheep atrial myocytes stained with di-4-ANEPPS. Figure 1Ai shows a cell with very few obvious t-tubules; however, this type of cell was very rare (2 of 42 cells). The majority of cells showed prominent t-tubules as demonstrated by the examples shown in Figure 1Bi and Ci. The right hand panels (Aii, Bii, and Cii) show calculated transverse (y-z) sections from the cells; t-tubules can be seen projecting into the interior of the cell from the cell surface. Figure 1D shows a calculated 2- $\mu\text{m}$  thick section from the same cell as Figure 1Ci. This shows the full length of many tubules which move in and out of the plane of focus in the thin section of Figure 1C. It also gives some idea of the number of t-tubules in a distance roughly equivalent to the sarcomere spacing. We have also made similar measurements on rat atrial cells and, in agreement with previous work,<sup>10,15</sup> find a complete absence of t-tubules with only sparse longitudinal elements<sup>8</sup> seen in some cells.

**Quantitative Analysis of Atrial T-Tubules**

The function of t-tubules is to ensure that elements inside the cell are nearer to the surface membrane than would be the case for a cell with no t-tubules. Therefore, to assess the potential quantitative importance of t-tubules one needs to see how close a given point in the cell is to the nearest t-tubule compared with the surface membrane. We have quantified this by measuring the distance from each point in the cell to the nearest element of membrane including both t-tubules and the rest of the surface membrane. A specimen output is shown in Figure 2Aii. Here, the intensity codes for the distance of each voxel of the cell from the nearest membrane. It is clear that some voxels in the section (dark areas on the distance map) are closer to membranes than are others. There are some regions (eg, within the circle in Figure 2A) where no t-tubules are seen in the section (Figure 2Ai), nevertheless the distance

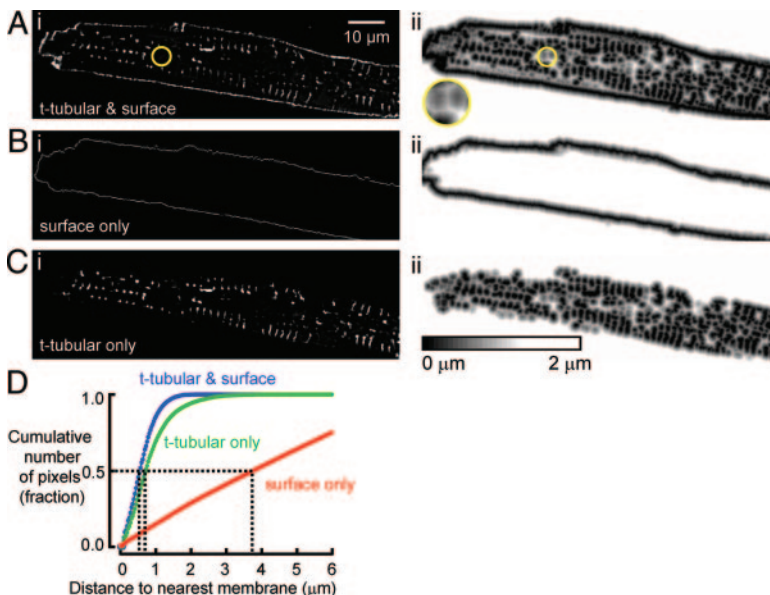


**Figure 2.** Measurement of proximity of t-tubules and surface membrane to voxels within a sheep atrial myocyte. A, Deconvolved image of a cell (i) and a distance map indicating the distance from any voxel to the nearest membrane (t-tubule or surface) (ii) are shown. The yellow circle highlights (and magnifies) a region where t-tubule staining is absent in the plane of focus yet clearly shows proximity to membrane in the distance map. B, Surface membrane (i) and distance map reporting distance to surface membrane (ii). C, t-tubules only (i) and distance map reporting distances to t-tubules (ii). D, Distance plot. The dotted lines show that 50% of voxels within the cell are less than the indicated distance from the nearest membrane. The colored lines correspond to images A–C: the blue line (A) shows distance to the nearest membrane either t-tubular or surface, the red line (B) to the nearest surface membrane, and the green line (C) to the nearest t-tubular membrane. The 10- $\mu\text{m}$  scale bar in Ai also applies to panels i and ii in A–C.

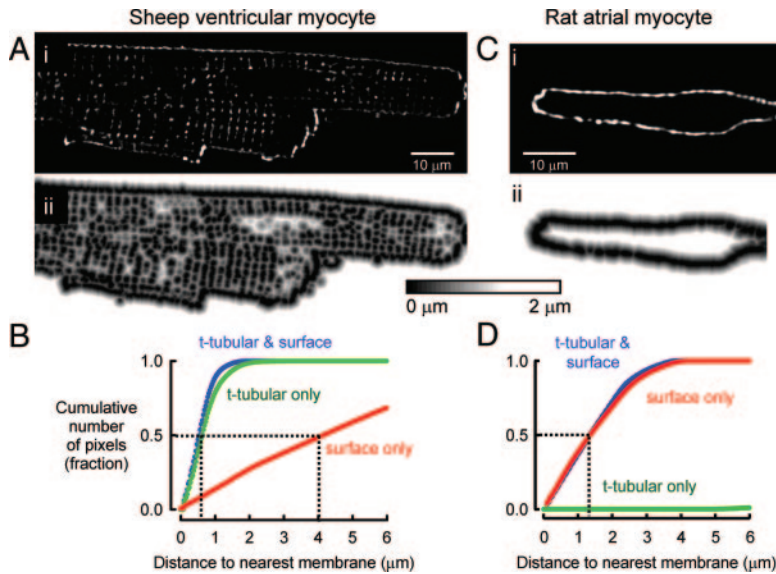


**Figure 3.** Comparative measurements on sheep ventricular and rat atrial myocytes. A, Sheep ventricular cell showing deconvolved image (i) and distance map (ii). B, Distance plot showing contributions of t-tubule and surface membrane. C, Rat atrial cell showing deconvolved image (i) and distance map (ii). D, Distance plot. The 10- $\mu\text{m}$  scale bars in Ai and Ci apply also to Aii and Cii, respectively.

measurements shown in Figure 2Aii demonstrate that these voxels are indeed close to membranes. This is because they are close to t-tubules in sections above or below the plane viewed here. The distance to membrane values are displayed graphically in Figure 2D, which shows the number of voxels in a cell that are less than a specified distance from the nearest membrane. For the example of Figure 2A, 50% of voxels are  $<0.57 \mu\text{m}$  (the “half-distance”) from the nearest membrane (blue line labeled “t-tubular and surface”). Figure 2D also shows the relative contributions of surface membrane alone and t-tubules alone to these distance plots. These latter components have been obtained by digitally removing, respectively, the t-tubule component (Figure 2B) or the surface sarcolemmal component (Figure 2C) and calculating the distance of each voxel within the cell to the nearest membrane. In Figure 2B, we have removed all fluorescence from the cell apart from the sarcolemma. As expected the majority of voxels in the cell are now much further from the nearest membrane as shown by the increase of bright areas in the distance map of Figure 2Bii. The red line of Figure 2D shows that, if only the sarcolemma is considered, 50% of voxels are now within  $3.78 \mu\text{m}$  from the nearest membrane, a distance far in excess of that where all membranes (surface sarcolemma and t-tubule) are included in the analysis (blue line in Figure 2D). For comparison, Figure 2C shows the cell with the surface membrane removed. It is clear both from the distance map of Figure 2Cii and the graph of Figure 2D (green line) that most voxels in the cell are much nearer to a t-tubule than they are to the surface membrane.

### T-Tubule Distribution in Sheep Ventricular and Rat Atrial Cells

Although there are many t-tubules in sheep atrial cells, their density still remains less than in the ventricle. The image of Figure 3Ai shows membrane staining for a typical sheep ventricular cell. Both this original image and the distance map of Figure 3Aii show that, although there is an extensive network of t-tubules, there are still regions with few tubules (Ai) and correspondingly large (bright) values on the distance

map (Aii). Applying similar distance analyses as in Figure 2 to the ventricular cell, the surface membrane only, t-tubule only and combined surface membrane and t-tubule contributions to the distance any voxel is from a cell membrane are summarized in Figure 3B. In this particular ventricular cell, the “half-distance” is  $0.54 \mu\text{m}$ . Most of this is due to t-tubules as shown by the near superposition of the t-tubular plus surface membrane line (blue) with that of t-tubules alone (green). For comparison, Figure 3C shows measurements from a typical rat atrial cell. Here, the absence of t-tubules means that the half-distance is  $1.35 \mu\text{m}$ . Furthermore, the curve for surface membrane only overlaps that for the t-tubule and sarcolemmal combined component clearly indicating that t-tubules do not contribute to the membrane—distance relationship (Figure 3D). Data for the contribution of each membrane component are summarized in Figure 4A. Considering sheep ventricular cells first, it is clear that the distance of any voxel in the cell from a membrane (surface sarcolemmal or t-tubule) is dominated by the presence of t-tubules as shown by the fact that, 50% of voxels are within  $0.54 \pm 0.06 \mu\text{m}$  of a t-tubule but  $4.35 \pm 0.22 \mu\text{m}$  from the nearest surface membrane (paired *t* test,  $P < 0.001$ ). At the other extreme, in the rat atrial cell, the surface sarcolemmal membrane predominates. Sheep atrial cells on the other hand are intermediate between sheep ventricular and rat atrial cells with the t-tubules being quantitatively far more important than the surface sarcolemma in minimizing the distance any voxel in the cell is from a membrane (surface sarcolemmal or t-tubule). Thus, in sheep atrial cells the half-distance to the nearest t-tubule membrane is  $1.42 \pm 0.10 \mu\text{m}$  compared with  $3.35 \pm 0.15 \mu\text{m}$  for the distance to the nearest surface sarcolemma (paired *t* test,  $P < 0.001$ ) and  $0.88 \pm 0.04 \mu\text{m}$  when all membranes are included.

An important consideration as to why there is such a profound difference in t-tubule structure between sheep and rat atrial cells is cell size. In the rat, atrial cells are thinner and shorter than ventricular cells.<sup>15</sup> In this study (Table) sheep atrial cells had mean length and width of  $126 \pm 2.75$  and  $15.2 \pm 1.48 \mu\text{m}$  ( $n = 23$  animals, 327 cells). This compares

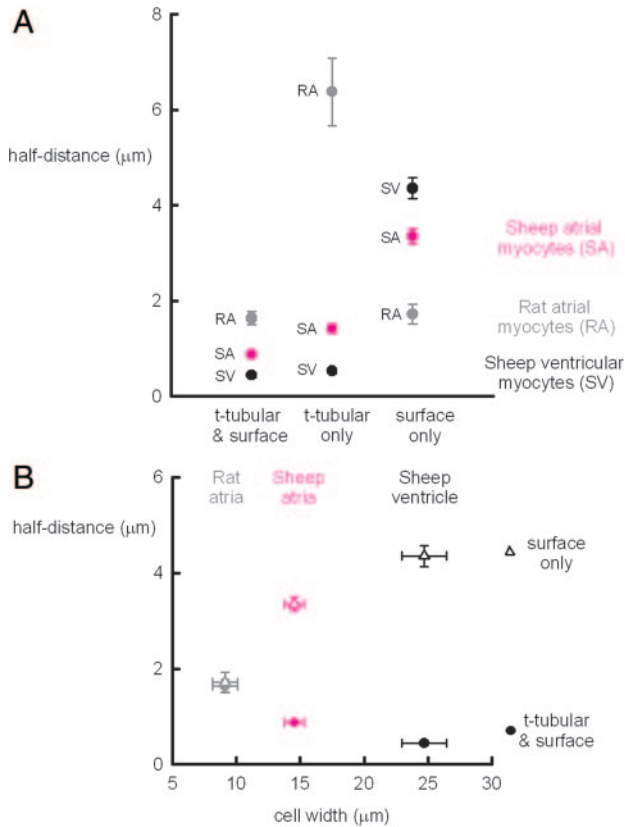


**Figure 4.** Half-distance of voxels in the cell from the nearest membrane. A, The 3 columns show half-distance of voxels in the cell from t-tubular and surface membrane, t-tubular membranes only, and surface membranes only. The half-distance is defined by 50% of pixels being closer to the membrane than this distance (see Figure 3). The symbols indicate rat atrium (RA), 8 cells; sheep atrium (SA), 42 cells; and sheep ventricle (SV), 12 cells. B, Data from A replotted as a function of cell width. For clarity, the points for distance to t-tubules only have been omitted.

with values of  $138.7 \pm 1.3$  and  $23.9 \pm 0.5$  μm for sheep ventricular cells (214 cells)<sup>25</sup> and  $83.0 \pm 5.4$  and  $9.5 \pm 0.5$  μm for rat atrial cells (22 cells).<sup>15</sup> The relationship between cell width and the distance to surface sarcolemmal or t-tubule membrane for each cell type is summarized in Figure 4B.

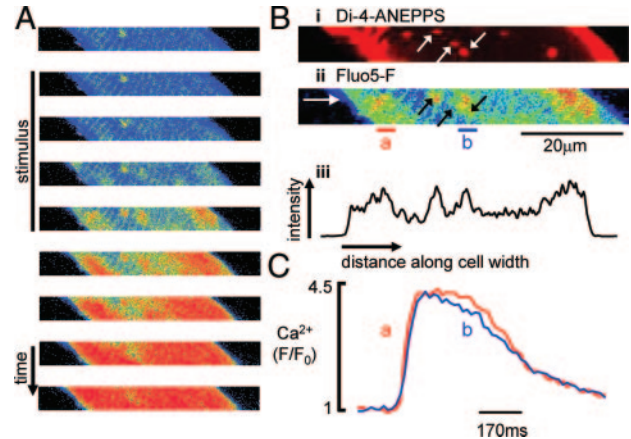


**Figure 5.** Correlation between t-tubules and intracellular release of  $Ca^{2+}$ . A, Consecutive x-y images (17-ms interval) showing  $[Ca^{2+}]_i$  measured using Fluo-5F. An external stimulus was applied for the period shown. B, di-4-ANEPPS staining (i) and the record of  $[Ca^{2+}]_i$  from the 5th frame in A is shown (ii). The 3 black arrows on the image of ii are in the same positions as the white arrows in i. The spatial distribution of  $[Ca^{2+}]_i$  along a horizontal line (iii) at the point, is indicated by the white arrow in ii. C, Specimen  $Ca^{2+}$  transients recorded from the periphery (a) and center (b). The measurements are from rectangular areas given by the whole height of the image and the horizontal lines at the positions indicated in Bii.

### Functional Role of Sheep Atrial T-Tubules in E-C Coupling

The next series of experiments addressed the functional significance of atrial t-tubules. Figure 5A shows the changes in  $[Ca^{2+}]_i$  on field stimulation of a sheep atrial cell. On stimulation, there is a simultaneous increase in  $[Ca^{2+}]_i$  at the cell periphery and regions of the cell interior, this is shown in Figure 5Biii and 5C. The correlation between the areas where  $[Ca^{2+}]_i$  rises synchronously on stimulation and presence of t-tubules is summarized in Figure 5B. After the measurement of  $[Ca^{2+}]_i$ , the cell was superfused with di-4-ANEPPS to identify t-tubules (Figure 5Bi). Comparing membrane staining (Figure 5Bi.) to the initial phase of the stimulated systolic  $Ca^{2+}$  transient (Figure 5Bii), it is clear that t-tubules are present in regions of the cell interior where  $[Ca^{2+}]_i$  rises immediately on stimulation. In 10 of 13 cells imaged in this

**Table. Cardiac Remodelling in Heart Failure**

|   | Control     | Heart Failure | Change, % | P                     |
|---|-------------|---------------|-----------|-----------------------|
| Left ventricular end-diastolic internal dimension, cm | 2.48 ± 0.10 | 3.84 ± 0.10   | +54.8     | $3 \times 10^{-6}$    |
| Left ventricular end systolic internal dimension, cm  | 0.82 ± 0.07 | 2.69 ± 0.10   | +228      | $2 \times 10^{-10}$   |
| Posterior wall thickness, cm                          | 1.12 ± 0.07 | 0.73 ± 0.04   | -34.8     | 0.0008                |
| M-mode fractional shortening                          | 0.64 ± 0.03 | 0.30 ± 0.02   | -53.1     | $< 1 \times 10^{-10}$ |
| Short-axis fractional area change                     | 0.67 ± 0.02 | 0.37 ± 0.02   | -44.8     | $1 \times 10^{-6}$    |
| Left atrial cell length, μm                           | 126 ± 2.75  | 169 ± 5.58    | +34.1     | $1.4 \times 10^{-8}$  |
| Left atrial cell width, μm                            | 15.1 (1.70) | 21.2 (5.81)   | +40.4     | 0.0001                |

Data are presented as mean ± SEM or median (interquartile range). Parameters assessed by echocardiography were performed in conscious animals with control measurements taken before surgery. n=14 animals per group, paired data (paired t test). For cell dimensions, n=9 (heart failure) to 22 (control) animals. Left atrial cell lengths were compared using the Student t test, whereas widths were compared using the Mann-Whitney rank-sum test.

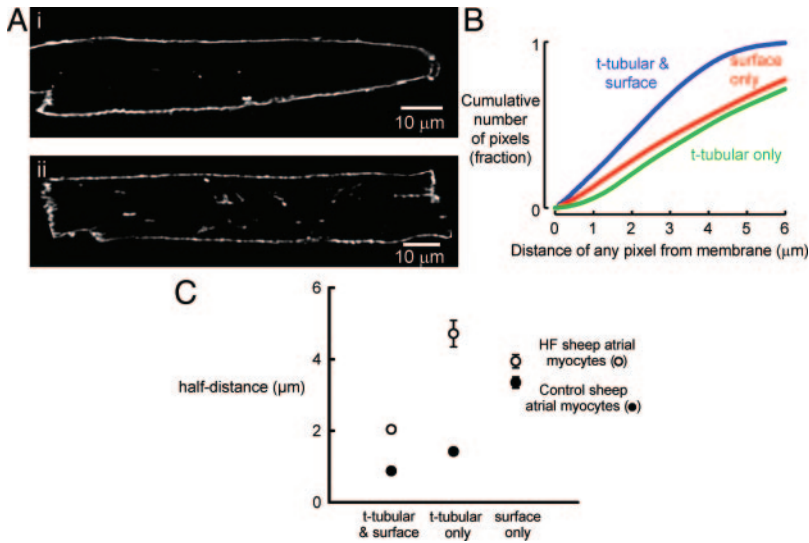


**Figure 6.** Loss of atrial t-tubules in heart failure (HF). A, Images from 2 representative cells from animals with heart failure. B, Distance plot showing distance of pixels in the cell from the various membranes. C, Summary data showing distance of voxels in the cell from various membranes for control (solid symbols) and HF (open). (Data from 29 cells).

manner, t-tubules were clearly present in the imaging plane used for  $[Ca^{2+}]_i$  measurements. In all of these cells the rise of  $[Ca^{2+}]_i$  occurred synchronously at the cell periphery and where the t-tubules were located.

**Cardiac Remodeling, Loss of Atrial T-Tubules, and Functional Consequences in Heart Failure**

Cardiac function was assessed before surgical implementation and immediately before sacrifice (pacing stopped 30 minutes before echocardiography). Changes in cardiac geometry and contractility were pronounced following 4 weeks of pacing. The Table summarizes the data; of particular note were a 54.8% increase in left ventricular end diastolic dimension and 53.1% decrease in LV fractional shortening ( $P=3 \times 10^{-6}$  and  $<1 \times 10^{-10}$ , respectively,  $n=14$  animals). Because of the anatomic arrangement of the LV apex and sternum in sheep, it is impossible using transthoracic echocardiography to obtain a 4 chamber apical view and therefore measurements of atrial dimensions. Compared with healthy controls, the atria were grossly dilated at the time of excision, an observation in agreement with the cellular hypertrophy in left atrial myocytes isolated from failing hearts (Table).

A typical left atrial cell isolated from a failing heart and stained with di-4-ANEPPS is shown in Figure 6Ai. T-tubules are virtually absent in the failing myocyte. Figure 6Aii shows an extreme example where intracellular staining is evident; however, even in this case, it is clear that t-tubules have a markedly altered distribution. We have quantified the distance to nearest membrane relationship for this cell (ie, Figure 6Ai) in Figure 6B. Summarizing the data (Figure 6C) shows that the loss of t-tubules results in an increase of half-distance from  $0.88 \pm 0.04 \mu m$  in control to  $2.04 \pm 0.08$  in heart failure (Mann-Whitney Rank Sum test, median 0.82 [interquartile range, 0.28] control and 2.05 [interquartile range, 0.49] heart failure,  $P < 0.001$ ).

$Ca^{2+}$  signaling was also markedly altered in heart failure as shown in Figure 7A. Here, the rise of  $[Ca^{2+}]_i$  initially occurred at the periphery of the cell before spreading into the interior. The 7th frame is shown in Figure 7Bii and the spatial distribution of  $[Ca^{2+}]_i$  emphasized in Figure 7Biii. The

peripheral initial increase of  $[Ca^{2+}]_i$  correlates with the lack of membrane staining in the interior of the cell. Finally, Figure 7C demonstrates the difference in the systolic  $Ca^{2+}$  transients from the periphery (a) and center (b) of the cell. We have measured  $Ca^{2+}$  signaling in 9 heart failure cells (from 4 animals). Seven of these cell showed the pattern of Figure 7 (rapid peripheral and slow central rise of  $[Ca^{2+}]_i$ ). Of the 2 which showed rapid rise of  $[Ca^{2+}]_i$  in some central locations, one had a t-tubule (shown by ANEPPS staining) in the image plane presumably accounting for the rapid rise and the other experiment ended before ANEPPS could be applied thus leaving open the possibility that there was a t-tubule remaining in the section.

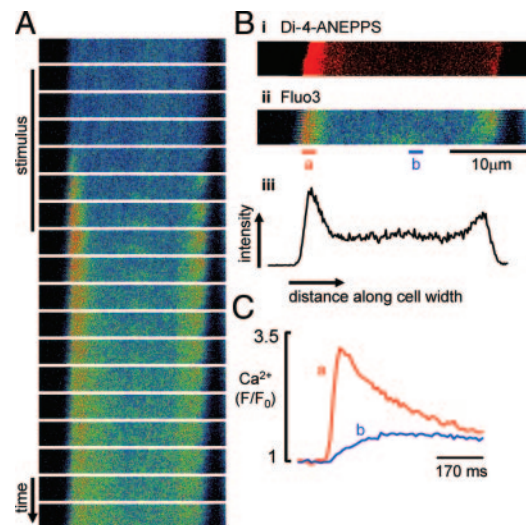


**Figure 7.** Spatial features of the  $Ca^{2+}$  transient in a myocyte from a heart failure sheep. A, Consecutive x-y images (17-ms interval) showing  $[Ca^{2+}]_i$  measured using Fluo-3. A stimulus was applied for the period shown. B, di-4-ANEPPS staining (i) is shown; and the record of  $[Ca^{2+}]_i$  from the 7th frame in A is shown (ii). The spatial distribution of  $[Ca^{2+}]_i$  from Bii is shown (iii). The mean fluorescence from the image is shown as a function of horizontal distance. C, Specimen  $Ca^{2+}$  transients recorded from the periphery (a) and center (b). The measurements are from rectangular areas given by the whole height of the image and the horizontal lines at the positions indicated in Bii.

## Discussion

The major findings of this article are (i) there is an extensive t-tubular system in the sheep atrium. This contrasts with previous work on the atria from smaller animals where the t-tubular system was either absent or rudimentary. (ii) In a model of heart failure with atrial dilatation, there is extensive disruption to, and loss of, atrial t-tubules. This extends previous work that has reported fractionation of t-tubules in failing ventricular cells. (iii) In normal sheep atrial cells, the  $\text{Ca}^{2+}$  transient rises rapidly at points in the interior of the cell near t-tubules and this rapid rise is absent, along with the t-tubules in heart failure.

A major function of t-tubules is to bring points inside the cell closer to the surface membrane. The t-tubules can be seen to play a major role to this effect in sheep atrial myocytes. Thus, Figure 4 shows that when all the data are considered, 50% of voxels in sheep atrial cells are less than  $0.88 \pm 0.04 \mu\text{m}$  from the nearest membrane (t-tubule or surface). If there were no t-tubules present then this distance would increase to  $3.35 \pm 0.15 \mu\text{m}$ . Rat atrial myocytes have no t-tubules and, in this context, it should be noted that rat atrial cells are smaller than those from sheep. The average width of rat atrial cells imaged for t-tubule membranes in this study is  $9.1 \pm 0.98 \mu\text{m}$  compared with  $14.5 \pm 0.75 \mu\text{m}$  for a sheep atrial cell (Figure 4B). The smaller size of the rat atrial cell means that, even without t-tubules, the distance at which 50% of voxels are from the nearest membrane is only  $1.72 \pm 0.21 \mu\text{m}$  thus meaning that there is less "need" for t-tubules in the rat atrium.

A major functional role for atrial t-tubules is demonstrated by the fact that, in contrast to smaller animals, the sheep atrium (where t-tubules are present) does not show a wave of  $\text{Ca}^{2+}$  release propagating radially into the cell. Rather,  $\text{Ca}^{2+}$  release can be observed at isolated points in the interior of the cell and colocalized to t-tubules. This may have implications for control of contractility in the sheep atrium as opposed to smaller animals. In the rat, for example, the systolic  $\text{Ca}^{2+}$  transient only occupies the periphery of the cell but, under inotropic stimulation, propagates to the center of the cell.<sup>27</sup> This study shows that, even in the absence of inotropic stimulation, the  $\text{Ca}^{2+}$  transient rises quickly in the center of the cell. It is therefore possible that inotropy in the sheep atrial myocyte results more from changes in the amplitude of the  $\text{Ca}^{2+}$  transient as opposed to its spatial distribution.

A striking observation in this work is the distinct loss of t-tubules from atrial myocytes in heart failure. This is similar to, but quantitatively more dramatic than the disruption to the ventricular t-tubular system in heart failure.<sup>21–24,28</sup> As a result of these changes, the distance at which 50% of voxels in a heart failure atrial cell reside from a membrane (t-tubule or surface sarcolemma) is now  $2.04 \pm 0.08 \mu\text{m}$  compared with  $0.88 \pm 0.04 \mu\text{m}$  in control cells. The bulk of this effect is due to the loss of t-tubules rather than an increase of cell dimensions (Figure 6). This loss of t-tubules is accompanied by gross changes in the spatial profile of the systolic  $\text{Ca}^{2+}$  transient (Figure 7). The transient thus rises rapidly only at the periphery of the cell and much more slowly in the interior.

Finally, this work has identified an extensive t-tubular system in the sheep atrial myocytes. Further work is needed to see whether this is typical of other large mammals including human. If so, this may have important implications in the control of excitation-contraction coupling in the atria under normal conditions and in disease states such as heart failure and atrial fibrillation.

## Acknowledgments

We acknowledge St Jude Medical for generous provision of hardware and Dr Christian Soeller (University of Auckland) for advice on computing.

## Sources of Funding

This work was supported by grants from the British Heart Foundation (including the Michael Frazer PhD Scholarship to J.D.C.), a European Union Specific Targeted REsearch Project ("NORMACOR," 6th Framework Programme), and Strategic Promotion of Ageing Research Capacity.

## Disclosures

Dr Dibb held a University of Manchester Stepping Stone Fellowship and is a British Heart Foundation Intermediate Fellow.

## References

1. Kannel WB, Wolf PA, Benjamin EJ, Levy D. Prevalence, incidence, prognosis, and predisposing conditions for atrial fibrillation: population-based estimates. *Am J Cardiol*. 1998;82:2N–9N.
2. Bootman MD, Higazi DR, Coombes S, Roderick HL. Calcium signalling during excitation-contraction coupling in mammalian atrial myocytes. *J Cell Sci*. 2006;119:3915–3925.
3. Brette F, Orchard C. Resurgence of cardiac t-tubule research. *Physiology (Bethesda)*. 2007;22:167–173.
4. Ayettey AS, Navaratnam V. The T-tubule system in the specialized and general myocardium of the rat. *J Anat*. 1978;127:125–140.
5. Brette F, Orchard C. T-tubule function in mammalian cardiac myocytes. *Circ Res*. 2003;92:1182–1192.
6. Hüser J, Lipsius SL, Blatter LA. Calcium gradients during excitation-contraction coupling in cat atrial myocytes. *J Physiol (Lond)*. 1996;494:641–651.
7. Hibbs RG, Ferrans VJ. An ultrastructural and histochemical study of rat atrial myocardium. *Am J Anat*. 1969;124:251–270.
8. Kirk MM, Izu LT, Chen-Izu Y, McCulle SL, Wier WG, Balke CW, Shorofsky SR. Role of the transverse-axial tubule system in generating calcium sparks and calcium transients in rat atrial myocytes. *J Physiol (Lond)*. 2003;547:441–451.
9. Woo SH, Cleemann L, Morad M. Diversity of atrial local  $\text{Ca}^{2+}$  signalling: evidence from 2-D confocal imaging in  $\text{Ca}^{2+}$ -buffered rat atrial myocytes. *J Physiol (Lond)*. 2005;567:905–921.
10. Brette F, Komukai K, Orchard CH. Validation of formamide as a detubulation agent in isolated rat cardiac cells. *Am J Physiol*. 2002;283:H1720–H1728.
11. Mackenzie L, Bootman MD, Berridge MJ, Lipp P. Predetermined recruitment of calcium release sites underlies excitation-contraction coupling in rat atrial myocytes. *J Physiol (Lond)*. 2001;530:417–429.
12. Blatter LA, Kocksammer J, Sheehan KA, Zima AV, Huser J, Lipsius SL. Local calcium gradients during excitation-contraction coupling and alternans in atrial myocytes. *J Physiol (Lond)*. 2003;546:19–31.
13. Brette F, Rodriguez P, Komukai K, Colyer J, Orchard CH. beta-adrenergic stimulation restores the  $\text{Ca}^{2+}$  transient of ventricular myocytes lacking t-tubules. *J Mol Cell Cardiol*. 2004;36:265–275.
14. Woo SH, Cleemann L, Morad M.  $\text{Ca}^{2+}$  current-gated focal and local  $\text{Ca}^{2+}$  release in rat atrial myocytes: evidence from rapid 2-D confocal imaging. *J Physiol (Lond)*. 2002;543:439–453.
15. Walden AP, Dibb KM, Trafford AW. Differences in intracellular calcium homeostasis between atrial and ventricular myocytes. *J Mol Cell Cardiol*. 2009;46:463–473.
16. Wijffels MC, Kirchhof CJ, Dorland R, Allessie MA. Atrial fibrillation begets atrial fibrillation. A study in awake chronically instrumented goats. *Circulation*. 1995;92:1954–1968.

17. Anne W, Willems R, Holemans P, Beckers F, Roskams T, Lenaerts I, Ector H, Heidbuchel H. Self-terminating AF depends on electrical remodeling while persistent AF depends on additional structural changes in a rapid atrially paced sheep model. *J Mol Cell Cardiol.* 2007;43:148–158.
18. Shi Y, Ducharme A, Li D, Gaspo R, Nattel S, Tardif JC. Remodeling of atrial dimensions and emptying function in canine models of atrial fibrillation. *Cardiovasc Res.* 2001;52:217–225.
19. Dolber PC, Bauman RP, Rembert JC, Greenfield JC Jr. Regional changes in myocyte structure in model of canine right atrial hypertrophy. *Am J Physiol Heart Circ Physiol.* 1994;267:H1279–H1287.
20. Melnyk P, Zhang L, Shrier A, Nattel S. Differential distribution of Kir2.1 and Kir2.3 subunits in canine atrium and ventricle. *Am J Physiol.* 2002; 283:H1123–H1133.
21. Louch WE, Mork HK, Sexton J, Stromme TA, Laake P, Sjaastad I, Sejersted OM. T-tubule disorganization and reduced synchrony of  $Ca^{2+}$  release in murine cardiomyocytes following myocardial infarction. *J Physiol.* 2006;574:519–533.
22. Balijepalli RC, Lokuta AJ, Maertz NA, Buck JM, Haworth RA, Valdivia HH, Kamp TJ. Depletion of T-tubules and specific subcellular changes in sarcolemmal proteins in tachycardia-induced heart failure. *Cardiovasc Res.* 2003;59:67–77.
23. Cannell MB, Crossman DJ, Soeller C. Effect of changes in action potential spike configuration, junctional sarcoplasmic reticulum micro-architecture and altered t-tubule structure in human heart failure. *J Muscle Res Cell Motil.* 2006;27:297–306.
24. Song LS, Sobie EA, McCulle S, Lederer WJ, Balke CW, Cheng H. Orphaned ryanodine receptors in the failing heart. *Proc Natl Acad Sci USA.* 2006;103:4305–4310.
25. Dibb KM, Rueckschloss U, Eisner DA, Isenberg G, Trafford AW. Mechanisms underlying enhanced cardiac excitation contraction coupling observed in the senescent sheep myocardium. *J Mol Cell Cardiol.* 2004; 37:1171–1181.
26. Soeller C, Cannell MB. Examination of the transverse tubular system in living cardiac rat myocytes by 2-photon microscopy and digital image-processing techniques. *Circ Res.* 1999;84:266–275.
27. Mackenzie L, Roderick HL, Berridge MJ, Conway SJ, Bootman MD. The spatial pattern of atrial cardiomyocyte calcium signalling modulates contraction. *J Cell Sci.* 2004;117:6327–6337.
28. Louch WE, Bito V, Heinzel FR, Macianskiene R, Vanhaecke J, Flameng W, Mubagwa K, Sipido KR. Reduced synchrony of  $Ca^{2+}$  release with loss of T-tubules—a comparison to  $Ca^{2+}$  release in human failing cardiomyocytes. *Cardiovasc Res.* 2004;62:63–73.

### CLINICAL PERSPECTIVE

Atrial fibrillation is the most common cardiac arrhythmia. Considerable evidence implicates changes of intracellular calcium in the genesis of atrial fibrillation, and it is therefore essential to understand atrial calcium signaling. However, compared with the better-studied ventricular myocyte, much less is known about atrial calcium cycling. Ventricular myocytes have a transverse tubular (t-tubular) system comprising invagination of the surface membrane, which allows calcium entry across the sarcolemma to reach points deep in the cell. Previous work showed that these t-tubules were absent in atrial cells from small laboratory animals, and this was correlated with the delayed appearance of the systolic calcium transient deep within the cell. We now show that sheep atrial myocytes have a well-ordered t-tubular system, and this is correlated with a rapid increase of calcium within the cell. In contrast, myocytes from animals in heart failure (produced by rapid ventricular pacing) show an almost complete loss of t-tubules and absence of the rapid increase of calcium within the cell. We speculate that the human atrial myocyte may have similar properties to that from the sheep, and therefore the observed changes of t-tubular structure and calcium handling may occur during human cardiac disease including atrial fibrillation.

### Characterization of an Extensive Transverse Tubular Network in Sheep Atrial Myocytes and its Depletion in Heart Failure

Katharine M. Dibb, Jessica D. Clarke, Margaux A. Horn, Mark A. Richards, Helen K. Graham,  
David A. Eisner and Andrew W. Trafford

*Circ Heart Fail.* 2009;2:482-489; originally published online July 29, 2009;  
doi: 10.1161/CIRCHEARTFAILURE.109.852228

*Circulation: Heart Failure* is published by the American Heart Association, 7272 Greenville Avenue, Dallas, TX  
75231

Copyright © 2009 American Heart Association, Inc. All rights reserved.  
Print ISSN: 1941-3289. Online ISSN: 1941-3297

The online version of this article, along with updated information and services, is located on the  
World Wide Web at:

<http://circheartfailure.ahajournals.org/content/2/5/482>

**Permissions:** Requests for permissions to reproduce figures, tables, or portions of articles originally published in *Circulation: Heart Failure* can be obtained via RightsLink, a service of the Copyright Clearance Center, not the Editorial Office. Once the online version of the published article for which permission is being requested is located, click Request Permissions in the middle column of the Web page under Services. Further information about this process is available in the [Permissions and Rights Question and Answer](#) document.

**Reprints:** Information about reprints can be found online at:  
<http://www.lww.com/reprints>

**Subscriptions:** Information about subscribing to *Circulation: Heart Failure* is online at:  
<http://circheartfailure.ahajournals.org/subscriptions/>